Eur. Phys. J. B **56**, 259–271 (2007)
DOI: 10.1140/epjb/e2007-00107-6

THE EUROPEAN PHYSICAL JOURNAL B

Self-similarity, small-world, scale-free scaling, disassortativity, and robustness in hierarchical lattices

Z.-Z. Zhang[a], S.-G. Zhou[b], and T. Zou

Department of Computer Science and Engineering, Fudan University, Shanghai 200433, P.R. China
and
Shanghai Key Lab of Intelligent Information Processing, Fudan University, Shanghai 200433, P.R. China

Received 16 December 2006 / Received in final form 28 February 2007
Published online 27 April 2007 –

Abstract. In this paper, firstly, we study analytically the topological features of a family of hierarchical lattices (HLs) from the view point of complex networks. We derive some basic properties of HLs controlled by a parameter q: scale-free degree distribution with exponent $\gamma = 2+\ln 2/(\ln q)$, null clustering coefficient, power-law behavior of grid coefficient, exponential growth of average path length (non-small-world), fractal scaling with dimension $d_B = \ln(2q)/(\ln 2)$, and disassortativity. Our results show that scale-free networks are not always small-world, and support the conjecture that self-similar scale-free networks are not assortative. Secondly, we define a deterministic family of graphs called small-world hierarchical lattices (SWHLs). Our construction preserves the structure of hierarchical lattices, including its degree distribution, fractal architecture, clustering coefficient, while the small-world phenomenon arises. Finally, the dynamical processes of intentional attacks and collective synchronization are studied and the comparisons between HLs and Barabási-Albert (BA) networks as well as SWHLs are shown. We find that the self-similar property of HLs and SWHLs significantly increases the robustness of such networks against targeted damage on hubs, as compared to the very vulnerable non fractal BA networks, and that HLs have poorer synchronizability than their counterparts SWHLs and BA networks. We show that degree distribution of scale-free networks does not suffice to characterize their synchronizability, and that networks with smaller average path length are not always easier to synchronize.

PACS. 89.75.Da Systems obeying scaling laws – 05.45.Df Fractals – 36.40.Qv Stability and fragmentation of clusters – 05.45.Xt Synchronization; coupled oscillators

1 Introduction

Topological characteristics, such as scale-free degree distribution, small-world effect, fractal scaling and degree correlations, have recently attracted much attention in network science. The last few years have witnessed a tremendous activity devoted to the characterization and understanding of networked systems [1–5]. Small-world property [6] and scale-free behavior [7] are two unifying concepts constituting our basic understanding of the organization of real-life complex systems. Small-world property refers to the one that the expected number of edges (links) needed to pass from one arbitrarily selected node (vertex) to another one is low, which grows at most logarithmically with the number of nodes. Scale-free behavior means the majority of nodes in a network have only a few connections to other nodes, whereas some nodes are connected to many other nodes in the network. This poses a fundamental question how these two characteristics are related. It has been observed that small-world property and scale-free behavior are not independent [8]: scale-free networks, normally, have extremely short average path length (APL), scaling logarithmically or slower with system size. Is this universal?

In fact, the above mentioned two properties (i.e. small-world property and scale-free behavior) do not provide sufficient characterizations of the real-world systems. It has been observed that real networks exhibit ubiquitous degree correlations among their nodes [9–15]. This translates in the observation that the degrees of nearest neighbor nodes are not statistically independent but mutually correlated in practically every network imaginable. Correlations play an important role in the characterization of network topology, and have led to a first classification of complex networks [12]. A series of recent measurements

[a] e-mail: zhangzz@fudan.edu.cn
[b] e-mail: sgzhou@fudan.edu.cn

indicate social networks are all assortative, while all biological and technological networks disassortative: in social networks there is a tendency for the hubs to be linked together, in biological and technological network the hubs show the opposite tendency, being primarily connected to less connected nodes. Correlations are now a very relevant issue, especially in view of the important consequences that they can have on dynamical processes taking place on networks [16–19].

Recently, it has been discovered by the application of a renormalization procedure that diverse real networks, such as the WWW, protein-protein interaction networks and metabolic networks, exhibit fractal scaling and topological self-similarity [20–24]. Fractal scaling implies that in a network the minimum number of node-covering boxes N_B of linear size ℓ_B scales with respect to ℓ_B as a power-law of N_B, with an exponent that is given by a finite fractal dimension d_B [20]. Self-similarity refers to the invariant scale-free distribution probability to find a node with degree k, $P(k) \sim k^{-\gamma}$, i.e. the exponent γ remains the same under the renormalization with different box sizes [20,25]. In complex networks, fractality and self-similarity do not always imply each other: a fractal network model is self-similar, while a self-similar network is not always fractal [24]. One can obtain the fractal dimension d_B by measuring the ratio of N_B over the total number of nodes N in the network, which satisfies $N_B/N \sim \ell_B^{-d_B}$. After renormalizing the networks, the degree $k_B(\ell_B)$ of a node in the renormalized network versus the largest degree k_{hub} inside the box that was contracted to one node with degree k_{hub} in the renormalization process exhibits a scaling behavior: $k_B(\ell_B) = s(\ell_B)k_{hub}$, where $s(\ell_B)$ is assumed to scale like $s(\ell_B) \sim \ell_B^{-d_k}$ with d_k being the degree exponent of the boxes. In self-similar scale-free networks, the relation between the three indexes γ, d_B and d_k satisfies $\gamma = 1 + d_B/d_k$ [20].

Correlations and topological fractality are important properties for many real-world complex systems. Then a natural fundamental question is raised how the two characteristics relate to each other. Recent researches [21,23] have shown that self-similar scale-free networks are not assortative, and the qualitative feature of disassortativity is scale-invariant under renormalization. Moreover, self-similarity and disassortativity of scale-free networks make such networks more robust against a sinister attack on nodes with large degree, as compared to the very vulnerable non fractal scale-free networks [21].

However, do small-world property and scale-free behavior always go along? How do systems have evolved into self-similar disassortative scale-free networks? How the dynamical processes such as intentional attack and synchronization are influenced by the topological fractality and disassortativity of scale-free networks? Such a series of important questions still remain open. To relate these questions, in this paper we therefore launch a study seeking a better understanding of the relations among these topological properties.

It is of interest to study above important questions with deterministic methods. Because of their strong advantages, deterministic network models have received much attention [26–40]. First, the method of generating deterministic networks makes it easier to gain a visual understanding of how networks are shaped, and how do different nodes relate to each other [26]; moreover, deterministic networks allow to compute analytically their topological properties, which have played a significant role, both in terms of explicit results and a guide to and a test of simulated and approximate methods [26–40]. On the other hand, deterministic networks can be easily extended to produce random variants which exhibit the classical characteristics of many real-life systems [41–45] .

Inspired by the above mentioned questions, here we first introduce a deterministic family of networks. These networks are called hierarchical lattices (HLs), which yield exact renormalization-group solutions [46–51]. From the perspective of complex network, we show that HLs are simultaneously scale-free, self-similar and disassortative, but lack the small-world property. Then we present a deterministic construction of a class of small-world hierarchical lattices (SWHLs), which preserve the basic structure properties including power law degree distribution, self-similarity, and disassortativeness, while lead to the small-world effect. Finally, we investigate the effects of network structures on the dynamics taking place in them.

This article is organized as follows. In Section 2, we introduce the construction of hierarchical lattices (HLs) and study their topological features including the degree distribution, moments, clustering coefficient, grid coefficient, self-similarity, degree correlations, and average path length (APL). The detailed exact derivation about APL is shown in Appendix A. In Section 3, we propose the deterministic construction of the small-world hierarchical lattices (SWHLs) and study their properties. In Section 4, attack tolerance of HLs is studied and the comparisons between HLs and Barabási-Albert (BA) networks are shown. In Section 5, we do a comparative investigation of synchronization in HLs, SWHLs and BA networks. Section 6 is devoted to our conclusions.

2 Hierarchical lattices

In this section, from topological perspective of complex networks, we present the construction and the basic properties such as degree distribution, clustering coefficient, average path length (APL), fractality, and correlations of the hierarchical lattices (HLs).

2.1 Construction of the lattice

The hierarchical lattices [49] are constructed in an iterative manner as shown in Figure 1. We denote the hierarchical lattices (networks) after t generations by $H(q,t)$, $q \geq 2$ and $t \geq 0$. The networks are constructed as follows: for $t = 0$, $H(q,0)$ is an edge connecting two points. For $t \geq 1$, $H(q,t)$ is obtained from $H(q,t-1)$. We replace each of the existing edges in $H(q,t-1)$ by the connected cluster of edges on the right of Figure 1. The growing process is

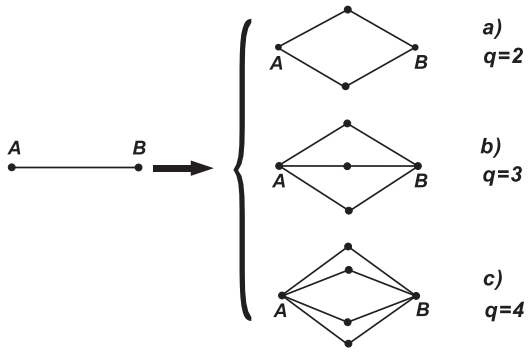

Fig. 1. Iterative construction method of the hierarchical lattices for some limiting cases.

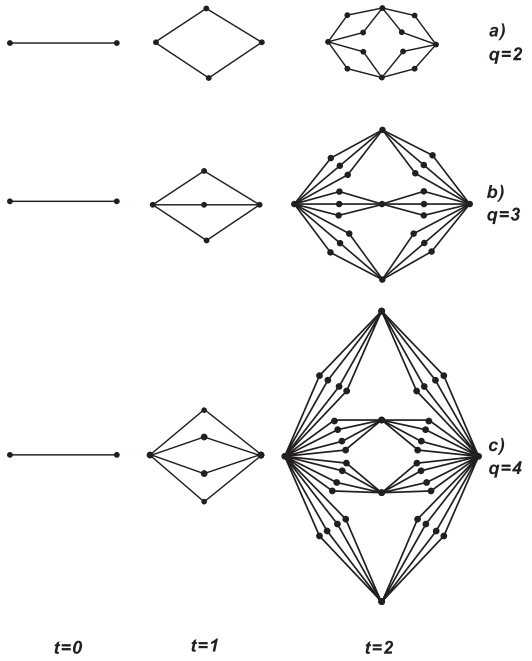

Fig. 2. Examples of the hierarchical lattices for some particular cases of $q = 2$, $q = 3$, and $q = 4$, showing the first three steps of the iterative process.

repeated t times, with the infinite lattices obtained in the limit $t \to \infty$. Figure 2 shows the growing process of the networks for three particular cases of $q = 2$, $q = 3$, and $q = 4$. It should be noted that in the hierarchical lattice of $q = 2$ case [46], the Migdal-Kadanoff [52,53] recursion relations with dimension 2 and length rescaling factor 2 are exact.

Griffiths and Kaufman provided two explanations for the construction of the hierarchical lattices [48], which are called "aggregation" and "miniaturization". In essence, these two interpretations reflect the self-similar structure of the hierarchical lattices, which allow one to calculate analytically their topological characteristics.

Next we compute the numbers of nodes (vertices) and links (edges) in $H(q,t)$. Let $L_v(t)$ and $L_e(t)$ be the numbers of vertices and edges created at step t, respectively. Note that each of the existing edges yields q nodes, and the addition of each new node leads to two new edges. By construction, for $t \geq 1$, we have

$$L_v(t) = qL_e(t-1) \tag{1}$$

and

$$L_e(t) = 2L_v(t). \tag{2}$$

Considering the initial condition $L_v(0) = 2$ and $L_e(0) = 1$, it follows that

$$L_v(t) = q\,(2q)^{t-1} \tag{3}$$

and

$$L_e(t) = (2q)^t. \tag{4}$$

Thus the number of total nodes N_t and edges E_t present at step t is

$$N_t = \sum_{t_i=0}^{t} L_v(t_i) = \frac{q(2q)^t + 3q - 2}{2q-1} \tag{5}$$

and

$$E_t = L_e(t) = (2q)^t, \tag{6}$$

respectively.

2.2 Degree distribution

Let $k_i(t)$ be the degree of node i at step t. Then by construction, it is not difficult to find following relation:

$$k_i(t) = q\,k_i(t-1), \tag{7}$$

which expresses a preferential attachment [7]. If node i is added to the network at step t_i, $k_i(t_i) = 2$ and hence

$$k_i(t) = 2\,q^{t-t_i}. \tag{8}$$

Therefore, the degree spectrum of the network is discrete. It follows that the degree distribution is given by

$$P(k) = \begin{cases} \dfrac{L_v(0)}{N_t} = \dfrac{2}{\frac{q(2q)^t+3q-2}{2q-1}} & \text{for } t_i = 0 \\ \dfrac{L_v(t_i)}{N_t} = \dfrac{q\,(2q)^{t_i-1}}{\frac{q(2q)^t+3q-2}{2q-1}} & \text{for } t_i \geq 1 \\ 0 & \text{otherwise} \end{cases} \tag{9}$$

and that the cumulative degree distribution [3,27] is

$$P_{\rm cum}(k) = \sum_{\rho \leq t_i} \frac{L_v(\rho)}{N_t} = \frac{q(2q)^{t_i} + 3q - 2}{q(2q)^t + 3q - 2}. \tag{10}$$

Substituting for t_i in this expression using $t_i = t - \frac{\ln \frac{k}{2}}{\ln q}$ gives

$$\begin{aligned} P_{\rm cum}(k) &= \frac{q\,(2q)^t \left(\frac{k}{2}\right)^{-\frac{\ln(2q)}{\ln q}} + 3q - 2}{q(2q)^t + 3q - 2} \\ &\approx \left(\frac{k}{2}\right)^{-(1+\frac{\ln 2}{\ln q})} \qquad \text{for large } t. \end{aligned} \tag{11}$$

So the degree distribution follows a power law behavior with the exponent $\gamma = 2 + \ln 2/(\ln q)$. For $q = 2$, equation (11) recovers the result of the particular case $p = 0$ previously obtained in reference [51].

$$\langle k^2\rangle_t = \begin{cases} \dfrac{4q(2q-1)}{q+\frac{3q-2}{(2q)^t}}\dfrac{q^t-2^t}{2^t(q^2-2q)}+\dfrac{2(2q-1)q^t}{q\cdot 2^t+\frac{3q-2}{q^t}} & \text{for } q>2 \\ \dfrac{4^t(3t+3)}{4^t+2} & \text{for } q=2 \end{cases}$$

$$\xrightarrow{t\to\infty} \begin{cases} \dfrac{4(q-1)(2q-1)}{q(q-2)}\left(\dfrac{q}{2}\right)^t & \text{for } q>2 \\ 3(t+1) & \text{for } q=2. \end{cases} \tag{15}$$

$$\langle k^3\rangle_t = \frac{2^{t+2}q^{3t+3}-2^{t+1}q^{3t+2}+2^{t+3}q^{3t+1}-2^{t+2}q^{3t}-2^{2t+4}q^{t+1}+2^{2t+3}q^t}{2^{2t}q^{t+3}-2^{2t+1}q^{t+1}+3\cdot 2^t q^3-3q\cdot 2^{t+1}-2^{t+1}q^2+2^{t+2}}. \tag{16}$$

2.3 Moments

Information on how the degree is distributed among the nodes of a undirected network can be obtained either by the degree distribution $P(k)$, or by the calculation of the moments of the distribution. The n-moment of $P(k)$ is defined as:

$$\langle k^n\rangle = \sum_k k^n P(k). \tag{12}$$

The first moment $\langle k\rangle$ is the mean degree. At arbitrary step t, the average vertex degree of $H(q,t)$ is

$$\langle k\rangle_t = \frac{2E_t}{N_t} = \frac{2(2q-1)(2q)^t}{q(2q)^t+3q-2}. \tag{13}$$

For large t, it is small and approximately equal to a finite value $4-2/q$.

We can also calculate higher moments of the distribution $P(k)$. For instance, the second moment, which measures the fluctuations of the connectivity distribution, is given by

$$\langle k^2\rangle_t = \frac{1}{N_t}\sum_{t_i=0}^{t} n_v(t_i)\left[k(t_i,t)\right]^2, \tag{14}$$

where $k(t_i,t)$ is the degree of a node at step t which was generated at step t_i. This quality expresses the average of degree square over all nodes in the network. It has large impact on the behavior of dynamical processes taking place in networks [54,55].

Substituting equations (3, 5, 8) into equation (14), we derive

see equation (15) above.

In this way, second moment of degree distribution $\langle k^2\rangle$ has been calculated explicitly, and the result shows that it becomes infinite for large t. In fact, because the degree exponent $\gamma \leq 3$, all n-moments ($n>2$) diverge. For example, we can analogously get the third moment as

see equation (16) above.

For the special case of $q=2$, it reduces to

$$\langle k^3\rangle_{q=2,t} = \frac{9\cdot 2^{3t}-6\cdot 2^{2t}}{2^{2t}+2}, \tag{17}$$

which diverges as an exponential law when t is very large.

2.4 Clustering coefficient

The clustering coefficient defines a measure of the level of cohesiveness around any given node. By definition, the clustering coefficient [6] C_i of node i is the ratio between the number of edges e_i that actually exist among the k_i neighbors of node i (i.e. the number of triangles attached to a vertex i) and its maximum possible value, $k_i(k_i-1)/2$, i.e., $C_i = 2e_i/k_i(k_i-1)$. The clustering coefficient of the whole network is the average of all individual $C_i's$.

Since there are no triangles in the hierarchial lattices, the clustering coefficient of every node and their average value in $H(q,t)$ are both zero by definition. However, over the years generalized clustering coefficients probing higher-order loops have been proposed [56,57]. Clearly in these hierarchial lattices the number of squares (loops of length 4) is significantly large, below we will seek to quantify this.

2.5 Grid coefficient

As pointed out above, for hierarchial lattices the usual clustering coefficient is unable to quantify the order underlying their structure, which is represented by a grid-like frame, that can be quantified by evaluating the frequency of rectangular loops (cycles of length 4). We introduce the *grid coefficient* that allows us to uncover the presence of a surprising level of triangular grid ordering in the hierarchial lattices. For simplicity, we call cycles of length 4 *quadrilaterals*. The grid coefficient [57] G_i of node i is defined as the ratio of number of existing quadrilaterals passing by node i, X_i, to all the possible number of quadrilaterals attached to node i, Y_i.

Note that each quadrilateral involving node i is consist of i itself plus three outer nodes, according to whose nature quadrilaterals can be classified, then the grid coefficient can be further decomposed into two cases (see Fig. 3): if all the outer nodes are directly attached to i, they form a *primary quadrilateral*; otherwise, if one of the outer nodes is a second neighbor of i, the cycle they form is a *secondary quadrilateral*. If a node i with degree k_i has $k_{i,2nd}$ second neighbors, then the maximum possible number of primary quadrilaterals is $Y_i^p = 3\times\binom{k_i}{3} = k_i(k_i-1)(k_i-2)/2$, while the maximum possible number of secondary quadrilaterals is $Y_i^s = k_{i,2nd}k_i(k_i-1)/2$. In this way, for investigating the grid properties of the hierarchial lattices, one

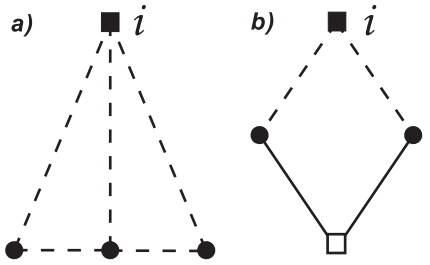

Fig. 3. (a) An example of a primary quadrilateral, where the three outer nodes are directly connected to node i. (b) An example of a secondary quadrilateral, where one outer node (empty square) is a second neighbor of node i.

can define three quantities: the primary grid coefficient, $G_i^p = X_i^p/Y_i^p$, the secondary grid coefficient $G_i^s = X_i^s/Y_i^s$, and the total grid coefficient $G_i = (X_i^p + X_i^s)/(Y_i^p + Y_i^s)$, where X_i^p and X_i^s are the actually existing number of primary and secondary quadrilaterals involving i, respectively. Averaging these quantities over all nodes, we can obtain the respective average grid coefficients.

There are only secondary quadrilaterals in HLs, so $G_i^p = 0$. The analytical expression for the secondary grid coefficient G_i^s of the individual node i with degree k can be derived exactly. In $H(q,t)$, for a node with degree great than two, there is a one-to-one correspondence between the second neighbors k_{2nd} of the node and its degree k: $k_{2nd} = k/q$. On the other hand, by construction, for a node with degree $k > 2$, for each of its second neighbor, there are just $\binom{q}{2}$ secondary quadrilaterals passing by the node and the second neighbor simultaneously, thus, the existing number of secondary quadrilaterals is $X^s = \frac{k}{q}\binom{q}{2}$. Therefore, for a node of degree $k > 2$, the exact value of its grid coefficient is

$$G(k) = \frac{q(q-1)}{k(k-1)}. \tag{18}$$

So the grid coefficient is a function of degree k, following a power-law behavior of the form k^{-2} for large k. It is interesting to note that a similar scaling has been observed in several real-life networks [57].

2.6 Fractality

In fact, the hierarchial lattices grow as a inverse renormalization procedure. To find the fractal dimension, we follow the mathematical framework proposed in reference [21]. By construction, for large t, the different quantities grow as:

$$\begin{cases} N_t \simeq 2q\, N_{t-1}, \\ k_i(t) = q\, k_i(t-1), \\ \mathbb{D}_t = 2\, \mathbb{D}_{(t-1)}. \end{cases} \tag{19}$$

The first equation is analogous to the multiplicative process naturally found in many population growth systems. The second relation denotes the preferential attachment mechanism [7], which yields the power law degree distribution. The third equation describes the change of the diameter $\mathbb{D}_t$ of the hierarchial lattices $H(q,t)$, where $\mathbb{D}_t$ is defined as by the longest shortest path between all pairs of nodes in $H(q,t)$.

From the relations given by equation (19), we know that these quantities N_t, $k_i(t)$ and $\mathbb{D}_t$ increase by a factor of $2q$, q and 2, respectively. Then between any two times t_1, t_2 ($t_1 < t_2$), we can easily obtain the following relation:

$$\begin{cases} \mathbb{D}_{t_2} = 2^{t_2-t_1}\, \mathbb{D}_{t_1}, \\ N_{t_2} = (2q)^{t_2-t_1}\, N_{t_1}, \\ k_i(t_2) = q^{t_2-t_1}\, k_i(t_1). \end{cases} \tag{20}$$

From equation (20), we can derive the scaling exponents in terms of the microscopic parameters: the fractal dimension is $d_B = \ln(2q)/(\ln 2)$, and the degree exponent of boxes is $d_k = \ln q/(\ln 2)$. The exponent of the degree distribution satisfies $\gamma = 1 + d_B/d_k = 2 + \ln 2/(\ln q)$, giving the same γ as that obtained in the direct calculation of the degree distribution, see equation (11).

Note that in a class of deterministic models called pseudo-fractals, although the number of their nodes increase exponentially, the additive growth in the diameter with time implies that these networks are small world. These models do not capture the fractal topology found in diverse complex networks [26–36].

2.7 Degree correlations

As the field of complex networks has progressed, degree correlations [9–15] have been the subject of particular interest, because they can give rise to some interesting network structure effects. Degree correlations can be conveniently measured by means of the conditional probability $P(k'|k)$, being defined as the probability that a link from a node of degree k points to a node of degree k'. In uncorrelated networks, this conditional probability does not depend on k, it takes the form $P(k'|k) = k'P(k')/\langle k\rangle$ [14].

Although degree correlations are formally characterized by $P(k'|k)$, the direct evaluation of the conditional probability $P(k'|k)$ in real-life systems is a very difficult task, and usually gives extremely noisy results because of their finite size. To overcome this problem, another interesting quantity related to two node correlations, called *average nearest-neighbor degree* (ANND), has been proposed. It is a function of node degree, and is more convenient and practical in characterizing degree-degree correlations, defined by [10]

$$k_{nn}(k) = \sum_{k'} k' P(k'|k). \tag{21}$$

If there are no degree correlations, equation (21) gives $k_{nn}(k) = \langle k^2\rangle/\langle k\rangle$, i.e. $k_{nn}(k)$ is independent of k. Degree correlations are usually quantified by reporting the numerical value of the slope of $k_{nn}(k)$ as a function of node degree k.

Degree correlations quantified by ANND have led to a first classification of complex networks. When $k_{\rm nn}(k)$ increases with k, it means that nodes have a tendency to

$$\bar{d}_t = \frac{1243\cdot 2^t - 475\cdot 2^{t+2}3^t + 275\cdot 2^{t+3}3^t + 275\cdot 2^t 3^{2t+1} + 19\cdot 2^{3t+2}3^{2t+1} - 11\cdot 3^{t+2}4^{t+1}}{44(2+2^t3^{t+1})(7+2^t3^{t+1})}$$

$$\overrightarrow{t\to\infty}\frac{19}{33}2^t, \tag{25}$$

connect to nodes with a similar or larger degree. In this case the network is defined as *assortative* [12,13]. In contrast, if $k_{\rm nn}(k)$ is decreasing with k, which implies that nodes of large degrees are likely to have the nearest neighbors with small degrees, then the network is said to be *disassortative*.

We can exactly calculate $k_{\rm nn}(k)$ for the hierarchial lattices. By construction, for nodes with degree greater than 2, the degrees of their neighbors are 2. Then we have

$$k_{\rm nn}(k>2) = 2. \tag{22}$$

For those nodes having degree 2, their average nearest-neighbor degrees are

$$k_{\rm nn}(2) = \frac{1}{2L_v(t)}\left(\sum_{t_i'=0}^{t_i'=t-1} L_v(t_i')\left[k(t_i',t)\right]^2\right) = \begin{cases} 2\,t & \text{for } q=2,\\ \dfrac{2q}{q-2}\left[\left(\dfrac{q}{2}\right)^t - 1\right] & \text{for } q>2. \end{cases} \tag{23}$$

Thus $k_{\rm nn}(2)$ grows linearly or exponentially with time for $q=2$ and $q>2$, respectively. As the nodes with degree 2 are only connected to higher degree nodes, $k_{\rm nn}(2)$ is significantly high.

Degree correlations can also be described by a Pearson correlation coefficient r of degrees at either end of a link. It is defined as [12,13,34,58]

$$r = \frac{\langle k\rangle\langle k^2 k_{\rm nn}(k)\rangle - \langle k^2\rangle^2}{\langle k\rangle\langle k^3\rangle - \langle k^2\rangle^2}. \tag{24}$$

If the network is uncorrelated, the correlation coefficient equals zero. Disassortative networks have $r<0$, while assortative graphs have a value of $r>0$. Substituting equations (8, 15, 16) into equation (24), we can easily see that for $t>1$, r of $H(q,t)$ is always negative, indicating disassortativity.

Disassortative features in protein interaction networks were found and explained by Maslov and Sneppen [9] on the level of interacting proteins and genetic regulatory interactions. According to their results links between highly connected nodes are systematically suppressed, while those between highly connected and low-connected pairs of proteins are favored.

2.8 Average path length

Shortest paths play an important role both in the transport and communication within a network and in the characterization of the internal structure of the network. We represent all the shortest path lengths of $H(q,t)$ as a matrix in which the entry d_{ij} is the geodesic path from node i to node j, where geodesic path is one of the paths connecting two nodes with minimum length. The maximum value of d_{ij} is called the diameter of the network. A measure of the typical separation between two nodes in the hierarchical lattices is given by the average path length $\bar{d}_t$, also known as characteristic path length, defined as the mean of geodesic lengths over all couples of nodes at the tth level.

For general q, it is not easy to derive a closed formula for the average path length $\bar{d}_t$ of $H(q,t)$. However, in Appendix A, we have obtained exact analytic expressions for $\bar{d}_t$ of $H(3,t)$, while the exact value of $\bar{d}_t$ of $H(2,t)$ has been obviously obtained in reference [51]. For $q=3$ we find

see equation (25) above.

leading to an exponential growth in the APL. Since in this case, $N_t\sim 6^t$ for large t, we have $\bar{d}_t\sim N_t^{\log_6 2}$. While in another special case $q=2$, $\bar{d}_t\sim N_t^{1/2}$ [51]. So for small q, the hierarchical lattices are not small worlds. We conjecture that for $H(q,t)$, their APL scales as $\bar{d}_t\sim N_t^{\log_{(2q)} 2}$, which is similar to that of a hypercubic lattice of dimension $\frac{1}{\log_{(2q)} 2}$. Low-dimensional regular lattices do not show the small-world behavior of typical node-node distances. It is straightforward to show that for a regular lattice in D dimensions which has the shape of a square or (hyper)cube of side l, and therefore has $N=l^D$ nodes, the APL increases as l, or equivalently as $N^{1/D}$ [59].

So we have shown that $\bar{d}_t$ of $H(q,t)$ has the power-law scaling behavior of the number of nodes N_t. It is not hard to understand. As an example, let us look at the scheme of the growth of a particular case $q=2$. Each next step in the growth of $H(2,t)$ doubles the APL between a fixed pair of nodes. The total numbers of nodes and edges increase four-fold (asymptotically, in the infinite limit of t), see equation (5). Thus the APL $\bar{d}_t$ of $H(2,t)$ grows as a square power of the node number in $H(2,t)$.

3 Small-world hierarchical lattices

In this section, we will discuss the construction and properties of small-world hierarchical lattices (SWHLs). Our goal is to reduce the diameter enough so as to get a logarithmically growing diameter, while maintaining the original structure of hierarchical lattices studied in the preceding section. All these can be attained by adding a new central point and connecting it with a certain set of original nodes, which is akin to the ideas presented in references [60–62].

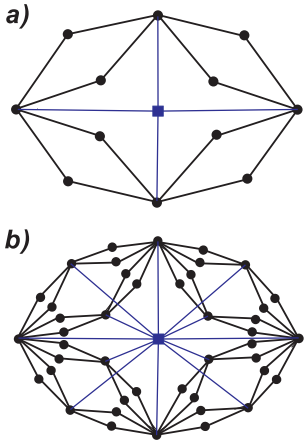

Fig. 4. (Color online) Construction of the small-world hierarchical lattices, with (a), (b) denoting $SH_1(2,2)$ and $SH_2(2,3)$, respectively.

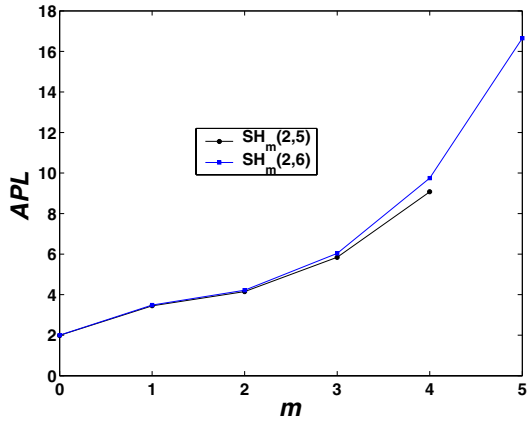

Fig. 5. (Color online) The dependence of average path length (APL) of $SH_m(2,5)$ and $SH_m(2,6)$ on m. One can see that APL increases very quickly as m grows.

We denote the small-world hierarchical lattices as $SH_m(q,t)$. From the previous section, we can know that for every $t \geq 2$ and $m = 1, 2, 3, ..., t-1$, $H(q,t)$ can be seen as $(2q)^{t-m}$ copies of $H(q,m)$, with some node identifications. $SH_m(q,t)$ $(1 \leq m \leq t-1)$ is the graph obtained by joining a new node to every hub (node of highest degree) of every copy of $H(q,m)$, see Figure 4. In other words, the new node is connected to those old nodes introduced at step $t-m$ or earlier, thus the number of new edges is exactly the number of vertices of $H(q,t-m)$. For $m = 0$, the new graph is out of the scope of $SH_m(q,t)$. In this case, for simplicity, we also denote the new network $SH_m(q,t)$, where the central node connects to all the nodes in $H(q,t)$.

The diameter of this new graph depends on the value of m. We will show that, for some of the values of m, the diameter of $SH_m(q,t)$ exhibits a slow (logarithmic) increase with the total number of network nodes. Thus, this construction gives us small-world graphs. Next we give the properties of small-world hierarchical lattices.

The order (number of all nodes) of $SH_m(q,t)$ is one plus the order of $H(q,t)$. The size (number of all edges) of $SH_m(q,t)$ is the size of $H(q,t)$, plus the number of added edges. Since the number of added edges is the order of $H(q,t-m)$, according to equations (5) and (6), we can easily see that the order and size of $SH_m(q,t)$ is $N_{m,t} = \frac{q(2q)^t+5q-3}{2q-1}$ and $E_{m,t} = \frac{(2q)^{t+1}-(2q)^t+q(2q)^{t-m}+3q-2}{2q-1}$, respectively.

Because the addition of the new node has little effect on the degree distribution, $SH_m(q,t)$ also follow power law degree distribution with the same degree exponent γ as $H(q,t)$. Additionally, for any $m \geq 1$, $SH_m(q,t)$ have no triangles, the clustering coefficient is zero as their counterparts $H(q,t)$. Analogously, $SH_m(q,t)$ are self-similar with the identical fractal dimension d_B as $H(q,t)$ [21,62].

Different from $H(q,t)$, $SH_m(q,t)$ have small-world property. For the sake of convenient expression, let us denote by $Diam[H(q,t)]$ the diameter of $H(q,t)$ and by $Diam[SH_m(q,t)]$ the diameter of $SH_m(q,t)$. Obviously, $Diam[H(q,t)] = 2^t$ [51]. To compute $Diam[SH_m(q,t)]$ we need only observe that, in $H(q,m)$, every node is at distance at most $Diam[H(q,m)]/2 = 2^{m-1}$ from the set of vertices of the hubs [62]. An upper bound for $Diam[SH_m(q,t)]$ is $Diam[H(q,m)] + 2 = 2^m + 2$. It can easily be seen that this is also a lower bound. Therefore, $Diam[SH_m(q,t)] = 2^m + 2$. Since the order $N_{m,t}$ of $SH_m(q,t)$ is $\frac{q(2q)^t+5q-3}{2q-1}$, if $m \leq \log_2 t$, then $Diam[SH_m(q,t)] \leq t + 2$ is small and scales logarithmically with the number of network nodes. Here we do not give the exact expression for the average path length (APL) of $SH_m(q,t)$, instead in Figure 5 we present APL of $SH_m(q,t)$ as a function of m. It is shown that APL becomes larger as m is increased.

To summarize, in the section, we proposed a construction of small-world hierarchical lattices. In the construction of these small-world lattices, the underlying structure of the original lattices is preserved. We have shown that all of these new graphs are fractal and have a logarithmic diameter.

4 Relative robustness to intentional attacks

As discussed in previous section, close to many real-life networks, the hierarchical lattices are simultaneously self-similar and scale-free. Therefore, it is worthwhile to investigate the processes taking place upon them and directly compare these results with just scale-free networks (like BA networks). These comparisons may give us deep insight into the dynamic properties of networks. In the following we will investigate intentional damage (attack) and synchronization, respectively. This section is devoted to the robustness, while next section is concerned with collective synchronization behavior.

Robustness refers to the ability of a network to avoid malfunctioning when a fraction of its constituents is damaged. This is a topic of obvious practical reasons, as it affects directly the efficiency of any process running on top of the network, and it is one of the first issues to be explored in the literature on complex networks [63]. Here

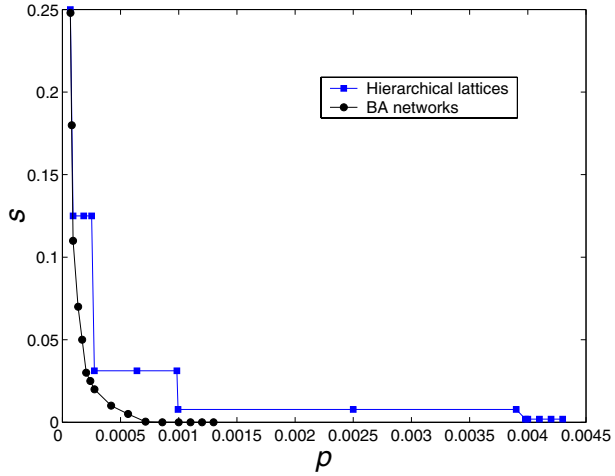

Fig. 6. (Color online) Vulnerability under intentional attack of a BA network with average degree 4 and a $H(2,8)$. Both networks have the same degree exponent ($\gamma = 3$), the same number of nodes (43, 692), and their clustering coefficient is small. Moreover, by construction, $SH_m(2,8)$ have similar robustness as $H(2,8)$, which rule out the effect of average path length on targeted attack. Thus, the difference in the resilience seen in this figure is attributed to fractality and the different degree of anticorrelations.

we shall focus only on the topological aspects (especially self-similarity) of robustness, caused by targeted removal of nodes, because there is a strong correlation between robustness and network topology [63–67].

One of the most important measures of the robustness of a network is its integrity, which is characterized by the presence of its giant connected component [63]. We call a network robust if it contains a giant cluster comprised of most of the nodes even after a fraction of its nodes are removed. Then, to know network robustness, first of all, one must study the variation of the giant component.

For the study of attack vulnerability of the network, the selection procedure of the order in which vertices are removed is an open choice [67]. One may of course maximize the destructive effect at any fixed number of removed vertices. However, this requires the knowledge of the whole network structure, and pinpointing the vertex to attack in this way makes a very time-demanding computation. A more tractable choice is to select the vertices in the descending order of degrees in the initial network and then to remove vertices one by one starting from the vertex with the highest degree; this attack strategy will be used in the present paper.

Figure 6 shows the performances of BA and hierarchial lattices under intentional attack. We plot the relative size of the largest cluster, s, after removing a fraction p of the largest hubs for both networks. One can find that the non-fractal scale-free BA networks are more sensitive to sabotage of a small fraction of the nodes, leading support to the view of Song et. al. [21]. While both networks collapse at a finite fraction p_c, evidenced by the decrease of s toward zero, the fractal network has a significantly larger threshold ($p_c \approx 0.004$) compared to the non-fractal threshold ($p_c \approx 0.001$), the former threshold is about 4 times than the latter, suggesting a significantly higher robustness of the fractal networks to intentional attacks. Also, it is interesting to note that for the hierarchical lattices, s is a function of p with a staircase-like form.

It is not strange at all that a giant connected component in self-similar networks is robust against the targeted deletion of nodes, while non-fractal scale-free networks are extremely vulnerable to targeted attacks on the hub. In non-fractal topologies, the hubs are connected and form a central compact core, such that the removal of a few of the largest hubs has catastrophic consequences for the network. In self-similar networks, hubs are more dispersed (see Fig. 2), their disassortativity and self-similar property significantly increases the robustness against targeted attacks. This could explain why some real-life networks have evolved into a fractal and disassortative architecture [20,21].

5 Synchronization

The ultimate goal of the study of network structure is to study and understand the workings of systems built upon those networks. Recently, along with the study of purely structural and evolutionary properties [1,2], there has been increasing interest in the interplay between the dynamics and the structure of complex networks [3–5]. One particular issue attracting much attention is the synchronizability of oscillator coupling networks [68]. Synchronization is observed in diverse natural and man-made systems and is directly related to many specific problems in a variety of different disciplines. It has found practical applications in many fields including communications, optics, neural networks and geophysics [69–74]. After studying the relevant characteristics of network structure, which is described in the previous sections, we will study the synchronization behavior on the networks.

We follow the general framework proposed in [75,76], where a criterion based on spectral techniques was established to determine the stability of synchronized states on networks. Consider a network of N identical dynamical systems with linearly and symmetric coupling between oscillators. The set of equations of motion for the system are

$$\dot{\mathbf{x}}_i = \mathbf{F}(\mathbf{x}_i) + \sigma \sum_{j=1}^{N} G_{ij}\mathbf{H}(\mathbf{x}_j), \qquad (26)$$

where $\dot{\mathbf{x}}_i = \mathbf{F}(\mathbf{x}_i)$ governs the dynamics of each individual node, $\mathbf{H}(\mathbf{x}_j)$ is the output function and σ the coupling strength, and G_{ij} is the Laplacian matrix, defined by $G_{ii} = k_i$ if the degree of node i is k_i, $G_{ij} = -1$ if nodes i and j are connected, and $G_{ij} = 0$ otherwise.

Since matrix G is positive semidefinite and each rows of it has zero sum, all eigenvalues of G are real and nonnegative and the smallest one is always equal to zero. We order the eigenvalues as $0 = \lambda_1 \leq \lambda_2 \leq ... \leq \lambda_N$. Then one can use the ratio of the maximum eigenvalue λ_N to the

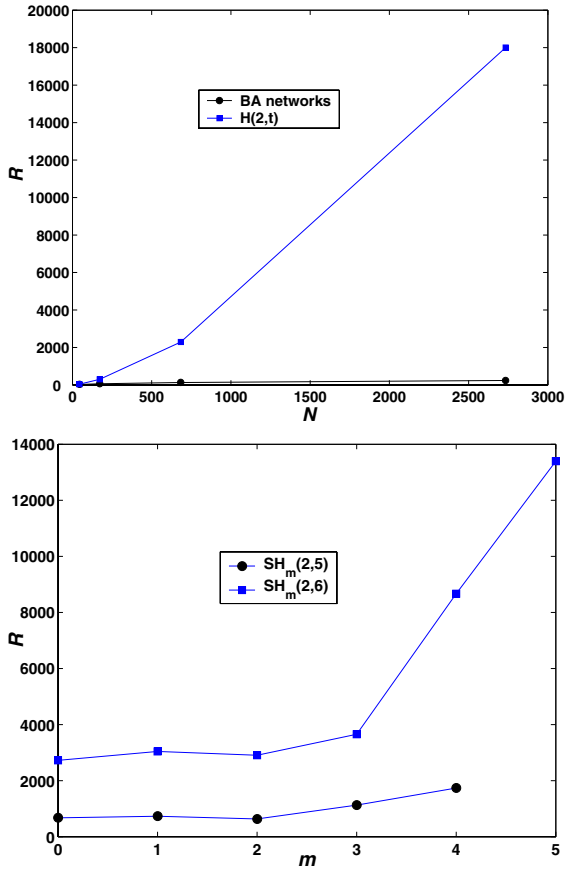

Fig. 7. (Color online) (Top) The eigenratio R as a function of network order N for BA networks with average degree 4 and $H(2,t)$. All quantities for BA networks are averaged over 50 realizations. (Bottom) The dependence of eigenratio R of $SH_m(2,5)$ and $SH_m(2,6)$ on the value of m.

smallest nonzero one λ_2 to measure the synchronizability of the network [75,76]. If the eigenratio $R = \lambda_N/\lambda_2$ satisfies $R < \alpha_2/\alpha_1$, we say the network is synchronizable. Here the eigenratio R depends on the the network topology, while α_2/α_1 depends exclusively on the dynamics of individual oscillator and the output function. Ratio $R = \lambda_N/\lambda_2$ represents the synchronizability of the network: the larger the ratio, the more difficult it is to synchronize the oscillators, and vice versa.

After reducing the issue of synchronizability to finding eigenvalues of the Laplacian matrix G, we now investigate the synchronization of our networks. Figure 7 shows the synchronizability of $H(2,t)$, $SH_m(2,5)$, $SH_m(2,6)$, as well as the BA networks. One can see that for the same network order, R of the BA networks is much smaller than that of hierarchical lattices $H(2,t)$, which implies that the synchronizability of the former is much better. While for $SH_m(2,5)$ and $SH_m(2,6)$, the dependence relation of eigenratio $R(m)$ on m is more complicated: $R(0) < R(2) < R(1) < R(x|x > 2)$; for $m > 2$, $R(m)$ increases with $m > 2$.

Why coupling systems on the BA networks, $H(2,t)$ and $SH_m(2,t)$ exhibit very different synchronizability? Previously reported results have indicated that underlying network structures play significant roles in the synchronizability of coupled oscillators. However, the key structural feature that determines the collective synchronization behavior remains unclear. Many works have discussed this issue. Some authors believe that shorter APL tends to enhance synchronization [75,77,78]. In contrast, Nishikawa et al. reported that synchronizability is suppressed as the degree distribution becomes more heterogeneous, even for shorter APL [79]. In reference [80], the authors asserted that larger average node degree corresponds to better synchronizability.

All these may rationally explain the relations between synchronizability and network structure in some cases, but do not well account for the difference of synchronizability between the graphs under consideration: as known from the preceding section, for fixed t, the APL of $SH_m(2,t)$ increases with m, but R does not always decrease with m; BA networks and $H(2,t)$ have identical degree exponent γ, while their synchronizability differs very much; in addition, the average degree of $SH_1(2,t)$ is higher than that of $SH_2(2,t)$, but the former is more difficult to synchronize than the latter. All these show that the degree distribution is generally not sufficient to characterize the synchronizability of scale-free networks [81,82], and that smaller average path length does not necessarily predict better synchronizability [82]. We speculate that the synchronizability on BA networks is better than on $H(2,t)$ and $SH_m(2,t)$ rests mainly with the self-similar structure. The genuine reasons need further research.

6 Conclusions

In conclusion, we have studied a family of deterministic networks called hierarchical lattices (HLs) from the perspective of complex networks. The deterministic self-similar construction allow one to derive analytic exact expressions for the relevant features of HLs. Our results shows that HLs exhibit many interesting topological properties: they follow a power-law degree distribution with exponent tuned from 2 to 3; their clustering coefficient is null but their grid coefficient follows a power-law phenomenon; they are not small-world, the APL scales like a power-law in the number of nodes; they have a fractal topology with a general fractal dimension; and they are disassortative networks. Our results indicate it is not true that a power-law degree alone create small-world networks [83], and further support the conjecture that scale-free networks with fractal scaling are disassortative. The disassortativity property is ease to understand by checking the growth process of HLs, where the rich (large nodes) get richer but at the expense of the poor (small nodes). In other words, the hubs prefer to grow by connections with less-connected nodes rather to other hubs, which leads to disassortativity. So we have found a good example — hierarchical lattices — which show that self-similar scale-free networks are preferably disassortative in their degree-degree correlations.

We have also introduced a deterministic construction of a family of small-world hierarchical lattices (SWHLs) and investigated their topological characteristics. We have shown that the some basic structure features of the hierarchical lattices (HLs) are preserved, including degree distribution, clustering coefficient and fractality, while the small-world phenomenon arises.

In addition, we have studied the dynamical processes such as intention damage and collective synchronization and have shown the comparisons between HLs and BA networks as well as SWHLs. We have found that self-similarity and disassortativity increase the robustness of networks under intentional attacks. Some qualitative explanations have been given showing that a fractal and disassortative topology structure is more robust. Although HLs and SWHLs have relative better robustness, they exhibit poorer synchronizability than BA networks based possibly on the same reasons as that of their insensitiveness to sabotage. We have shown that synchronizability of scale-free networks is not an intrinsic property of the exponent of degree distribution, and that small APL does not imply good synchronizability.

In future, it would be worth searching for other stochastic networks displaying finite fractal dimension spectra. Moreover, it is more interesting that the presence of self-similarity and disassortativity, as well as the absence of small-world properties of the HLs might have a relevant effect on the other dynamic process such as epidemic spreading [84], routing traffic [85,86], games [87] and transport [88] taking place on the networks.

This research was supported by the National Natural Science Foundation of China under Grant Nos. 60496327, 60573183, and 90612007, and the Postdoctoral Science Foundation of China under Grant No. 20060400162.

Appendix A: Derivation of the average path length for q = 3

We denote the set of nodes constituting the hierarchical lattices $H(q,t)$ after t construction steps as $L_{q,t}$. Then the APL for $L_{q,t}$ is defined as:

$$\bar{d}_t = \frac{D_t}{N_t(N_t-1)/2}\,, \tag{A.1}$$

where

$$D_t = \sum_{i\neq j,\ i\in L_{q,t},\, j\in L_{q,t}} d_{ij} \tag{A.2}$$

denotes the sum of the chemical distances between two nodes over all pairs, and d_{ij} is the chemical distance between nodes i and j. Although there are some difficulties in obtaining a closed formula for $\bar{d}_t$ holding true for all q, the hierarchical lattices have a self-similar structure that allows one to calculate $\bar{d}_t$ analytically according to different q. As shown in Figure A.1, the lattice $L_{q,t+1}$ may be obtained by joining $2q$ copies of $L_{q,t}$ at the hubs, which are labeled as $L_{q,t}^{(\alpha)}$, $\alpha = 1, 2, ..., 2q$. Then we can write the sum D_{t+1} as

$$D_{t+1} = 2q\, D_t + \Delta_t, \tag{A.3}$$

where Δ_t is the sum over all shortest paths whose endpoints are not in the same $L_{q,t}$ branch. The solution of equation (A.3) is

$$D_t = (2q)^{t-1} D_1 + \sum_{m=1}^{t-1} (2q)^{t-m-1} \Delta_m. \tag{A.4}$$

The paths that contribute to Δ_t must all go through at least one of the $q+2$ edge nodes (for $q = 3$ see Figure A.1, where $\boldsymbol{A}$, $\boldsymbol{B}$, $\boldsymbol{C}$, $\boldsymbol{D}$, $\boldsymbol{E}$ are the five edge nodes) at which the different $L_{q,t}$ branches are connected. The analytical expression for Δ_t for general q, called the crossing paths, is not easy to derive. We trace the formula only for the particular case of $q = 3$ as follows.

In what follows, we write $L_{3,t}$ as L_t for brevity. Denote $\Delta_t^{\alpha,\beta}$ as the sum of all shortest paths with endpoints in $L_t^{(\alpha)}$ and $L_t^{(\beta)}$. If $L_t^{(\alpha)}$ and $L_t^{(\beta)}$ meet at an edge node, $\Delta_t^{\alpha,\beta}$ rules out the paths where either endpoint is that shared edge node. If $L_t^{(\alpha)}$ and $L_t^{(\beta)}$ do not meet, $\Delta_t^{\alpha,\beta}$ excludes the paths where either endpoint is any edge node. Then the total sum Δ_t is

$$\begin{aligned}\Delta_t = \ & \Delta_t^{1,2} + \Delta_t^{1,3} + \Delta_t^{1,4} + \Delta_t^{1,5} + \Delta_t^{1,6} + \Delta_t^{2,3} \\ & + \Delta_t^{2,4} + \Delta_t^{2,5} + \Delta_t^{2,6} + \Delta_t^{3,4} + \Delta_t^{3,5} + \Delta_t^{3,6} \\ & + \Delta_t^{4,5} + \Delta_t^{4,6} + \Delta_t^{5,6} - 5\cdot 2^{t+1}.\end{aligned} \tag{A.5}$$

The last term at the end compensates for the overcounting of certain paths: the shortest path between $\boldsymbol{A}$ and $\boldsymbol{B}$, with length 2^{t+1}, is included in $\Delta_t^{1,6}$, $\Delta_t^{2,5}$ and $\Delta_t^{3,4}$; the shortest path between $\boldsymbol{C}$ and $\boldsymbol{E}$, with length 2^{t+1}, is included in both $\Delta_t^{1,3}$ and $\Delta_t^{4,6}$; the shortest path between $\boldsymbol{D}$ and $\boldsymbol{E}$, with length 2^{t+1}, is included in both $\Delta_t^{2,3}$ and $\Delta_t^{4,5}$; the shortest path between $\boldsymbol{C}$ and $\boldsymbol{D}$, also with length 2^{t+1}, is included in both $\Delta_t^{1,2}$ and $\Delta_t^{5,6}$.

By symmetry, $\Delta_t^{1,2} = \Delta_t^{1,3} = \Delta_t^{2,3} = \Delta_t^{5,6} = \Delta_t^{4,5} = \Delta_t^{4,6} = \Delta_t^{1,6} = \Delta_t^{2,5} = \Delta_t^{3,4}$ and $\Delta_t^{1,4} = \Delta_t^{1,5} = \Delta_t^{2,4} = \Delta_t^{2,6} = \Delta_t^{3,5} = \Delta_t^{3,6}$, so that

$$\Delta_t = 9\Delta_t^{1,2} + 6\Delta_t^{1,4} - 5\cdot 2^{t+1}, \tag{A.6}$$

where $\Delta_t^{1,2}$ is given by the sum

$$\begin{aligned}\Delta_t^{1,2} &= \sum_{i\in L_t^{(1)},\ j\in L_t^{(2)},\, i\neq A,\, j\neq A} d_{ij} \\ &= \sum_{i\in L_t^{(1)},\ j\in L_t^{(2)},\, i\neq A,\, j\neq A} (d_{iA} + d_{Aj}) \\ &= (N_t-1)\sum_{i\in L_t^{(1)}} d_{iA} + (N_t-1)\sum_{j\in L_t^{(2)}} d_{Aj} \\ &= 2(N_t-1)\sum_{i\in L_t^{(1)}} d_{iA}\,,\end{aligned} \tag{A.7}$$

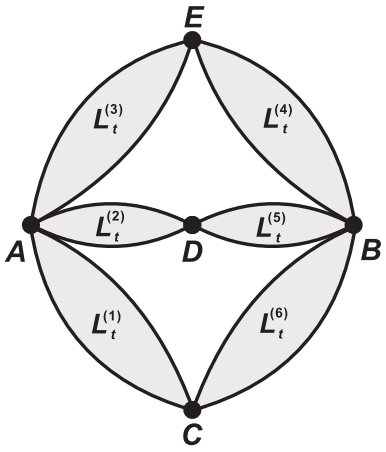

Fig. A.1. For $q = 3$, the hierarchical lattice after $t + 1$ construction steps, L_{t+1}, is composed of six copies of L_t denoted as $L_t^{(\chi)}$ $(\chi = 1, 2, \cdots, 6)$, which are connected to one another as above.

where $\sum_{i\in L_t^{(1)}} d_{iA} = \sum_{j\in L_t^{(2)}} d_{Aj}$ have been used. To find $\sum_{i\in L_t^{(1)}} d_{iA}$, we examine the structure of the hierarchical lattice at the tth level. In $L_t^{(1)}$, there is $\nu_t(m)$ points with $d_{iA} = m$, where $1 \le m \le 2^t$, and $\nu_t(m)$ can be written recursively as

$$\nu_t(m) = \begin{cases} 3^t & \text{if } m \text{ is odd} \\ \nu_{t-1}(\frac{m}{2}) & \text{if } m \text{ is even.} \end{cases} \tag{A.8}$$

We can write $\sum_{i\in L_t^{(1)}} d_{iA}$ in terms of $\nu_t(m)$ as

$$f_t \equiv \sum_{i\in L_t^{(1)}} d_{iA} = \sum_{m=1}^{2^t} m \cdot \nu_t(m). \tag{A.9}$$

Equation (A.8) and (A.9) relate f_t and f_{t-1}, which allow one to resolve f_t by induction as follow:

$$\begin{aligned} f_t &= \sum_{k=1}^{2^{t-1}} (2k-1)3^t + \sum_{k=1}^{2^{t-1}} 2k \cdot \nu_{t-1}(k) \\ &= 3^t 2^{2t-2} + 2f_{t-1} \\ &= \frac{1}{5} 2^{t-2}(14 + 6^{t+1}), \end{aligned} \tag{A.10}$$

where $f_1 = \nu_1(1) + 2\nu_1(2) = 5$ has been used. Substituting equation (A.10) and $N_t = \frac{7+3\times 6^t}{5}$ into equation (A.7), we obtain

$$\Delta_t^{1,2} = \frac{1}{25} 2^{t-1}(3 \times 6^t + 2)(6^{t+1} + 14). \tag{A.11}$$

Continue analogously,

$$\begin{aligned} \Delta_t^{1,4} &= \sum_{i\in L_t^{(1)},\ j\in L_t^{(4)}, i\neq A,C,\ j\neq B,E} d_{ij} \\ &= \sum_{i\in L_t^{(1)}, j\in L_t^{(4)}, i\neq A,\ j\neq E,\ d_{iA}+d_{jE}<2^t} (d_{iA} + 2^t + d_{jE}) \\ &\quad + \sum_{i\in L_t^{(1)}, j\in L_t^{(4)}, i\neq C,\ j\neq B,\ d_{iC}+d_{jB}<2^t} (d_{iC} + 2^t + d_{jB}) \\ &\quad + \sum_{i\in L_t^{(1)},\ j\in L_t^{(4)}, i\neq A,\ j\neq E,\ d_{iA}+d_{jE}=2^t} 2^{t+1}. \end{aligned} \tag{A.12}$$

The first term equal the second one and are denoted by g_t, and the third term is denoted by h_t, so that $\Delta_t^{1,4} = 2g_t + h_t$. One can compute the quantity g_t as

$$\begin{aligned} g_t &= \sum_{m=1}^{2^t-2} \sum_{m'=1}^{2^t-1-m} \nu_t(m)\nu_t(m')(m + 2^t + m') \\ &= \sum_{k=1}^{2^{t-1}-2} \sum_{k'=1}^{2^{t-1}-1-k} \nu_{t-1}(k)\nu_{t-1}(k')(2k + 2^t + 2k') \\ &\quad + \sum_{k=1}^{2^{t-1}-1} \sum_{k'=1}^{2^{t-1}-k} \nu_{t-1}(k)3^t(2k + 2^t + 2k' - 1) \\ &\quad + \sum_{k=1}^{2^{t-1}-1} \sum_{k'=1}^{2^{t-1}-k} 3^t\nu_{t-1}(k')(2k - 1 + 2^t + 2k') \\ &\quad + \sum_{k=1}^{2^{t-1}-1} \sum_{k'=1}^{2^{t-1}-k} 3^{2t}(2k - 1 + 2^t + 2k' - 1). \end{aligned} \tag{A.13}$$

The fourth terms can be summed directly, yielding

$$3^{2t}2^{t-3}(2^t - 2)^2 + 3^{2t-1}2^{t-1}(2^{t-1} + 1)(2^t - 2). \tag{A.14}$$

In equation (A.13), the second and third terms are equal to each other and can be simplified by first summing over k', yielding

$$3^t \textstyle\sum_{k=1}^{2^{t-1}-1} \nu_{t-1}(k)(3 \cdot 2^{2t-2} - 2^t k - k^2). \tag{A.15}$$

For use in equation (A.15), $\sum_{k=1}^{2^{t-1}-1} \nu_{t-1}(k) = N_{t-1} - 2$, and using equation (A.10),

$$\begin{aligned} \sum_{k=1}^{2^{t-1}-1} k\nu_{t-1}(k) &= \textstyle\sum_{k=1}^{2^{t-1}} k\nu_{t-1}(k) - 2^{t-1} \\ &= 2^{t-3}(6^t - 6)/5. \end{aligned} \tag{A.16}$$

Similarly to equation (A.10), we get

$$\sum_{k=1}^{2^{t-1}-1} k^2\nu_{t-1}(k) = \frac{1}{5}4^{t-1}6^{t-1} - \frac{1}{2}6^{t-1} + \frac{3}{10}4^{t-1}. \tag{A.17}$$

With these results, equation (A.15) becomes

$$\frac{1}{2}3^t(2 \cdot 4^{t-1}6^{t-1} - 3 \cdot 4^{t-1} + 6^{t-1}). \tag{A.18}$$

With equations (A.14) and (A.18), equation (A.13) becomes

$$g_t = 2g_{t-1} + \tfrac{1}{6}3^t6^t4^t - \tfrac{1}{6}3^t6^t - \tfrac{3}{4}3^t4^t + 2^{t-3}4^t9^t - \tfrac{1}{2}4^t9^t + \tfrac{1}{2}2^t9^t. \quad (A.19)$$

Considering the initial condition $g_1 = 0$, we can solve equation (A.19) inductively leading to

$$g_t = -\tfrac{3}{85}2^{t-3}(-171 + 17\cdot 2^{t+2}3^{t+1} + 5\cdot 2^{t+3}3^{2t+1} - 85\cdot 9^t - 17\cdot 4^{t+1}9^t). \quad (A.20)$$

To find an expression for $\Delta_t^{1,4}$, now the only thing left is to evaluate h_t as

$$\begin{aligned} h_t &= 2^{t+1}\sum_{m=1}^{2^t-1}\nu_t(m)\nu_t(2^t-m) \\ &= 2^{t+1}\sum_{m=1}^{2^t-1}\nu_t^2(m) \\ &= 2^{t+1}\left[\sum_{k=1}^{2^{t-1}}9^t + \sum_{k=1}^{2^{t-1}-1}\nu_{t-1}^2(k)\right] \\ &= 6^{2t} + 2h_{t-1}\,, \end{aligned} \quad (A.21)$$

where we have used the the symmetry $\nu_t(m) = \nu_t(2^t - m)$. Since $h_1 = 36$, equation (A.21) is solved inductively:

$$h_t = \frac{9}{17}2^{t+1}(18^t - 1). \quad (A.22)$$

From equations (A.20) and (A.22),

$$\Delta_t^{1,4} = -\frac{3}{85}2^{t-2}(-171 + 17\cdot 2^{t+2}3^{t+1} + 5\cdot 2^{t+3}3^{2t+1} - 85\cdot 9^t - 17\cdot 4^{t+1}9^t) + \frac{9}{17}2^{t+1}(18^t - 1). \quad (A.23)$$

Substituting equations (A.11) and (A.23) into equation (A.6), we obtain the final expression for the crossing paths Δ_t:

$$\begin{aligned} \Delta_t = {} & \frac{9}{25}2^{t-1}(2 + 3\cdot 6^t)(14 + 6^{t+1}) \\ & - \frac{9}{85}2^{t-1}(-171 + 17\cdot 2^{t+2}3^{t+1} \\ & + 5\cdot 2^{t+3}3^{2t+1} - 85\cdot 9^t - 17\cdot 4^{t+1}9^t) \\ & + \frac{54}{17}2^{t+1}(18^t - 1) - 5\cdot 2^{t+1}. \end{aligned} \quad (A.24)$$

Substituting equations (A.24) for Δ_m into equation (A.4), and using $D_1 = 14$, we have

$$D_t = \frac{1}{2200}(1243\cdot 2^t - 475\cdot 2^{t+2}3^t + 275\cdot 2^{t+3}3^t + 275\cdot 2^t3^{2t+1} + 19\cdot 2^{3t+2}3^{2t+1} - 11\cdot 3^{t+2}4^{t+1}) \quad (A.25)$$

Inserting equation (A.25) into equation (A.1), one can obtain the analytical expression for $\bar{d}_t$ in equation (25).

References

1. R. Albert, A.-L. Barabási, Rev. Mod. Phys. **74**, 47 (2002)
2. S.N. Dorogvtsev, J.F.F. Mendes, Adv. Phys. **51**, 1079 (2002)
3. M.E.J. Newman, SIAM Rev. **45**, 167 (2003)
4. S. Boccaletti, V. Latora, Y. Moreno, M. Chavez, D.-U. Hwanga, Phys. Rep. **424**, 175 (2006)
5. K. Borner, S. Sanyaland, A. Vespignani, Ann. Rev. Infor. Sci. Tech. **41**, 537 (2007)
6. D.J. Watts, H. Strogatz, Nature (London) **393**, 440 (1998)
7. A.-L. Barabási, R. Albert, Science **286**, 509 (1999)
8. R. Cohen, S. Havlin, Phys. Rev. Lett. **90**, 058701 (2003)
9. S. Maslov, K. Sneppen, Science **296**, 910 (2002)
10. R. Pastor-Satorras, A. Vázquez, A. Vespignani, Phys. Rev. Lett. **87**, 258701 (2001)
11. A. Vázquez, R. Pastor-Satorras, A. Vespignani, Phys. Rev. E **65**, 066130 (2002)
12. M.E.J. Newman, Phys. Rev. Lett. **89**, 208701 (2002)
13. M.E.J. Newman, Phys. Rev. E **67**, 026126 (2003)
14. M. Boguñá, R. Pastor-Satorras, Phys. Rev. E **68**, 036112 (2003)
15. A. Barrat, R. Pastor-Satorras, Phys. Rev. E **71**, 036127 (2005)
16. M. Boguñá, R. Pastor-Satorras, Phys. Rev. E **66**, 047104 (2002)
17. Y. Moreno, A. Vázquez, Eur. Phys. J. B **31**, 265 (2003)
18. A. Vázquez, Y. Moreno, Phys. Rev. E **67**, 015101 (2003)
19. P. Echenique, J. Gómev-Gardeñes, Y. Moreno, A. Vázquez, Phys. Rev. E **71**, 035102 (2003)
20. C. Song, S. Havlin, H.A. Makse, Nature **433**, 392 (2005)
21. C. Song, S. Havlin, H.A. Makse, Nature Phys. **2**, 275 (2006)
22. S.H. Strogatz, Nature (London) **433**, 365 (2005)
23. S.-H. Yook, F. Radicchi, H.M.-Ortmanns, Phys. Rev. E **72**, 045105 (2005)
24. K.I. Goh, G. Salvi, B. Kahng, D. Kim, Phys. Rev. Lett. **96**, 018701 (2006)
25. F.C. Zhao, H.J. Yang, B.H. Wang, Phys. Rev. E **72**, 046119 (2005)
26. A.-L. Barabási, E. Ravasz, T. Vicsek, Physica A **299**, 559 (2001)
27. S.N. Dorogovtsev, A.V. Goltsev, J.F.F. Mendes, Phys. Rev. E **65**, 066122 (2002)
28. F. Comellas, G. Fertin, A. Raspaud, Phys. Rev. E **69**, 037104 (2004)
29. Z.Z. Zhang, L.L. Rong, S.G. Zhou, Physica A **377**, 329 (2007)
30. S. Jung, S. Kim, B. Kahng, Phys. Rev. E **65**, 056101 (2002)
31. E. Ravasz, A.L. Somera, D.A. Mongru, Z.N. Oltvai, A.-L. Barabási, Science **297**, 1551 (2002)
32. E. Ravasz, A.-L. Barabási, Phys. Rev. E **67**, 026112 (2003)
33. J.S. Andrade Jr, H.J. Herrmann, R.F.S. Andrade, L.R. da Silva, Phys. Rev. Lett. **94**, 018702 (2005)
34. J.P.K. Doye, C.P. Massen, Phys. Rev. E **71**, 016128 (2005)
35. Z.Z. Zhang, F. Comellas, G. Fertin, L.L. Rong, J. Phys. A **39**, 1811 (2006)
36. Z.Z. Zhang, L.L. Rong, S.G. Zhou, Phys. Rev. E **74**, 046105 (2006)
37. F. Comellas, J. Ozón, J.G. Peters, Inf. Process. Lett. **76**, 83 (2000)
38. F. Comellas, M. Sampels, Physica A **309**, 231 (2002)

39. Z.Z. Zhang, L.L. Rong, C.H. Guo, Physica A **363**, 567 (2006)
40. T. Zhou, B.H. Wang, P.M. Hui, K.P. Chan, Physica A **367**, 613 (2006)
41. S.N. Dorogovtsev, J.F.F. Mendes, A.N. Samukhin, Phys. Rev. E **63**, 062101 (2001)
42. J. Ozik, B.-R. Hunt, E. Ott, Phys. Rev. E **69**, 026108 (2004)
43. Z.Z. Zhang, L.L. Rong, F. Comellas, J. Phys. A **39**, 3253 (2006)
44. T. Zhou, G. Yan, B.H. Wang, Phys. Rev. E **71**, 046141 (2005)
45. Z.Z. Zhang, L.L Rong, F. Comellas, Physica A **364**, 610 (2006)
46. A.N. Berker, S. Ostlund, J. Phys. C **12**, 4961 (1979)
47. M. Kaufman, R.B. Griffiths, Phys. Rev. B **24**, 496 (1981)
48. R.B. Griffiths, M. Kaufman, Phys. Rev. B **26**, 5022 (1982)
49. Z.R. Yang, Phys. Rev. B **38**, 728 (1988)
50. Y. Qin, Z.R. Yang, Phys. Rev. B **43**, 8576 (1991)
51. M. Hinczewski, A.N. Berker, Phys. Rev. E **73**, 066126 (2006)
52. A.A. Migdal, Zh. Eksp. Teor. Fiz. **69**, 1457 (1975) [Sov. Phys. JETP **42**, 743 (1976)]
53. L.P. Kadanoff, Ann. Phys. (N.Y.) **100**, 359 (1976)
54. R. Pastor-Satorras, A. Vespignani, Phys. Rev. Lett. **86**, 3200 (2001)
55. R. Pastor-Satorras, A. Vespignani, Phys. Rev. E **63**, 066117 (2001)
56. G. Bianconi, A. Capocci, Phys. Rev. Lett. **90**, 078701 (2003)
57. G. Caldarelli, R. Pastor-Satorras, A. Vespignani, Eur. Phys. J. B **38**, 183 (2004)
58. J.J. Ramasco, S.N. Dorogovtsev, R. Pastor-Satorras, Phys. Rev. E **70**, 036106 (2004)
59. M.E.J. Newman, J. Stat. Phys. **101**, 819 (2000)
60. S.N. Dorogovtsev, J.F.F. Mendes, Europhys. Lett. **50**, 1 (2000)
61. T. Nishikawa, A.E. Motter, Y.C. Lai, F.C. Hoppensteadt, Phys. Rev. E **66**, 046139 (2002)
62. L. Barriére, F. Comellas, C. Dalfó, J. Phys. A **39**, 11739 (2006)
63. R. Albert, H. Jeong, A.-L. Barabási, Nature (London) **406**, 378 (2000)
64. D.S. Callaway, M.E.J. Newman, S.H. Strogatz, D.J. Watts, Phys. Rev. Lett. **85**, 5468 (2000)
65. R. Cohen, K. Erez, D. ben-Avraham, S. Havlin Phys. Rev. Lett. **86**, 3682 (2001)
66. S.N. Dorogovtsev, J.F.F. Mendes, Phys. Rev. Lett. **87**, 219801 (2001)
67. P. Holme, B.J. Kim, C.N. Yoon, S.K. Han, Phys. Rev. E **65**, 056109 (2002)
68. S. Strogatz, *SYNC-How the emerges from chaos in the universe, nature, daily life* (Hyperion, New York, 2003)
69. L.M. Pecora, T.L. Carroll, Phys. Rev. Lett. **64**, 821 (1990)
70. H.G. Winful, L. Rahman, Phys. Rev. Lett. **65**, 1575 (1990)
71. D. Hansel, H. Sompolinsky, Phys. Rev. Lett. **68**, 718 (1992)
72. K.M. Cuomo, A.V. Oppenheim, Phys. Rev. Lett. **71**, 65 (1993)
73. M. de S. Vieira, Phys. Rev. Lett. **82**, 201 (1999)
74. K. Otsuka, Phys. Rev. Lett. **84**, 3049 (2000)
75. M. Barahona, L.M. Pecora, Phys. Rev. Lett. **89**, 054101 (2002)
76. L.M. Pecora, T.L. Carroll, Phys. Rev. Lett. **80**, 2109 (1998)
77. P.M. Gade, C.K. Hu, Phys. Rev. E **62**, 6409 (2000)
78. T. Zhou, M. Zhao, B.H. Wang, Phys. Rev. E **73**, 037101 (2006)
79. T. Nishikawa, A.E. Motter, Y.C. Lai, F.C. Hoppensteadt, Phys. Rev. Lett. **91**, 014101 (2003)
80. B.H. Gong, L. Yang, K.Q. Yang, Phys. Rev. E **72**, 037101 (2005)
81. F.M. Atay, T. Biyikoğlu, J. Jost, IEEE Trans. Circuits Syst., I: Fundam. Theory Appl. **53**, 92 (2006)
82. A. Hagberg, P.J. Swart, D.A. Schult, Phys. Rev. E **74**, 056116 (2006)
83. K. Klemn, V.M. Eguíluz, Phys. Rev. E **65**, 036123 (2002)
84. Z.Z. Zhang, S.G. Zhou, T. Zou (unpublished)
85. L. Zhao, Y.C. Lai, K. Park, N. Ye, Phys. Rev. E **71**, 026125 (2005)
86. W.X. Wang, C.Y. Yin, G. Yan, B.H. Wang, Phys. Rev. E **74**, 016101 (2006)
87. W.X. Wang, J. Ren, G.R. Chen, B.H. Wang, Phys. Rev. E **74**, 056113 (2006)
88. C.P. Zhu, S.J. Xiong, T. Chen, Phys. Rev. B **58**, 12848 (1998)